

Feed rate modeling in circular-circular interpolation discontinuity for high-speed milling

Bassem Gassara, Maher Baili, Gilles Dessen, Moncef Hbaieb, Wassila Bouzid Sai

► To cite this version:

Bassem Gassara, Maher Baili, Gilles Dessen, Moncef Hbaieb, Wassila Bouzid Sai. Feed rate modeling in circular-circular interpolation discontinuity for high-speed milling. *International Journal of Advanced Manufacturing Technology*, Springer Verlag, 2013, vol. 65, pp. 1619-1634. 10.1007/s00170-012-4284-z . hal-00959278

HAL Id: hal-00959278

<https://hal.archives-ouvertes.fr/hal-00959278>

Submitted on 14 Mar 2014

HAL is a multi-disciplinary open access archive for the deposit and dissemination of scientific research documents, whether they are published or not. The documents may come from teaching and research institutions in France or abroad, or from public or private research centers.

L'archive ouverte pluridisciplinaire **HAL**, est destinée au dépôt et à la diffusion de documents scientifiques de niveau recherche, publiés ou non, émanant des établissements d'enseignement et de recherche français ou étrangers, des laboratoires publics ou privés.



Open Archive TOULOUSE Archive Ouverte (OATAO)

OATAO is an open access repository that collects the work of Toulouse researchers and makes it freely available over the web where possible.

This is an author-deposited version published in : <http://oatao.univ-toulouse.fr/>
Eprints ID : 8655

To link to this article : <http://dx.doi.org/10.1007/s00170-012-4284-z>

To cite this version :

Gassara, Bassem and Baili, Maher and Dessein, Gilles and Hbaieb, Moncef and Bouzid Saï, Wassila *Feed rate modeling in circular–circular interpolation discontinuity for high-speed milling*. (2013) The International Journal of Advanced Manufacturing Technology, vol. 65 (n° 9 -12). pp. 1619-1634. ISSN 0268-3768

Any correspondance concerning this service should be sent to the repository administrator: staff-oatao@listes-diff.inp-toulouse.fr

Feed rate modeling in circular–circular interpolation discontinuity for high-speed milling

B. Gassara · M. Baili · G. Dessein · M. Hbaieb · W. Bouzid Saï

Abstract In this paper, a modeling approach is presented in order to evaluate feed rate during a circular interpolation in high-speed milling. The developed model depends on the type of discontinuity and the kinematic performance of the machine tool. To begin with, a feed rate modeling for circular interpolation with continuity in tangency is developed. After, the discontinuity in tangency between two circular interpolations is replaced by discontinuity in curvature by adding a fillet which is in relation to the functional tolerance ε imposed in the part design. An experimental study has been carried out to validate the models.

Keywords High-speed machining · Circular interpolation · Feed rate · Tangency and curvature discontinuity

Nomenclature

$V_{(t)}$	Instantaneous feed rate (in millimeter per minute)
V_{prog}	Programmed feed rate (in millimeter per minute)
V_m	Maximum feed rate (in millimeter per minute)
V_{Lb}	Feed rate limited by length of block (in millimeter per minute)
V_{icy}	Feed rate limited by t_{cy} (in millimeter per minute)
V_{An}	Feed rate limited by normal acceleration (in millimeters per minute)
V_{Jt}	Feed rate limited by tangential jerk (in millimeters per minute)
V_{fc}	Transition feed rate (in millimeters per minute)

$A_{(t)}$	Acceleration of work (in meters per square second)
A_m	Maximum acceleration (in meters per square second)
A_n	Normal acceleration (in meters per square second)
A_t	Tangential acceleration (in meters per square second)
$J_{(t)}$	Jerk of work (in meters per cubic second)
J_m	Maximum jerk (in meters per cubic second)
J_t	Tangential jerk (in meters per cubic second)
J_n	Normal jerk (in meters per cubic second)
t_{cy}	Interpolation cycle time (in seconds)
T_c	Simulated cycle time (in seconds)
T_{cCAM}	Cycle time calculated by CAM software (in seconds)
T_{acc}	Acceleration time (in seconds)
T_{dec}	Deceleration time (in seconds)
T_{Vprog}	Total time when we used V_{prog}
δt	Circular transition block crossing time (in seconds)
C_{act}	Actual cost
C_{est}	Estimated cost
C_m	Cost of the machine
S	Curvilinear abscissa (in millimeters)
$R_1; R_2$	Workpiece curvature radius (in millimeters)
R_C	Fillet radius (in millimeters)
ε	Imposed error (in millimeters)
γ	Orientation angle (in degrees) (<i>rad</i>)
r_1	The percentage of the use of V_{prog}

B. Gassara · M. Hbaieb · W. B. Saï
Unité de Génie de Production Mécanique et Matériaux, ENIS,
route Soukra Km 3.5,
B.P. 1173-3038 Sfax, Tunisia

B. Gassara (✉) · M. Baili · G. Dessein
LGP, INP/ENIT; Université de Toulouse,
47 avenue d'Azereix,
BP 1629, 65016 Tarbes, Cedex, France
e-mail: bassem.gassara@enit.fr

1 Introduction

Among the functions of the computer-aided manufacturing (CAM) software, we can find the creation of a tool path. Through this function, we can realize any requested operation. This trajectory is described by the software; it can be composed of many elementary interpolations shared in

linear (G01) and circular interpolation (G02 and G03). The large number of these elementary interpolations requires a variety of discontinuities in the path [1–4]. This will cause a significant instability in the real feed rate, which results in slowdowns at the end of each interpolation because the transition feed rate in discontinuities are much lower than the programmed feed rate [5–8]. This implies an increase in machining time and non compliance with the programmed feed rate [9, 10]. The real machining time is often very high compared to the time estimated by the CAM software, which leads to productivity issues and an underestimation of the cost of machining for the industry.

In the context of high-speed milling (HSM), primarily, it is necessary to adapt the tool path to rapid piloting the machine and to respect the maximum consumed power. To make the trajectories continuous, two methods are possible. The first is to add a circle arc in the crossing of discontinuity in tangency [6, 7, 11, 12]. The second is to estimate the trajectory with polynomial function [13]. Then, the machine must have a rigid structure adapted to these conditions. The performances, which are associated with the numerical control unit (interpolation cycle time, look ahead...), should be also improved.

Pessoles [6] has presented the fillet radius modeling on the level of discontinuities in tangency which was in relation with the surface tolerance ε . This modeling was applied to a path on linear–linear contour. In the manufacturing industries, the fillet radius is inserted through a discontinuity by using the NC functions G641 and G642. The latter permits to insert a fillet according to the distance which the rounding block may begin (G641) and the axial tolerance (G642). These two functions do not reflect the value of tolerance ε (as shown on Fig. 1).

In this paper, a model calculating the feed rate during a circular interpolation is presented. For the modeling, the tool path is discretized into several blocks with discontinuity in tangency and curvature (Fig. 1). The t.d. between two circular interpolations was replaced by curvature discontinuity (c.d.) by adding a fillet which is a function of the tolerance ε .

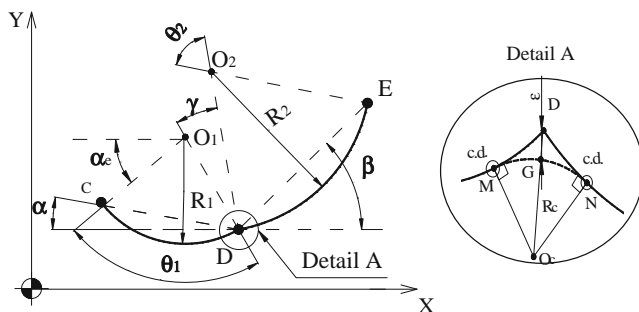


Fig. 1 Circular–circular contour

The establishment of this model allows us to identify the machine behavior at the transition between two circular interpolations and to determine the optimal fillet radius. For imposed machining quality (error ε), an optimization of cycle time is achieved through the determination of the optimal fillet radius R_c . This model can be applied in the machining strategies that contain circular interpolations. An experimental study was carried out on a HSM machine to verify the developed models.

2 Feed rate modeling for circular interpolation with continuity in tangency

The theoretical study was developed in two steps. The first step focuses on the feed rate modeling in circular interpolation. The second one was devoted to modeling geometric continuity in tangency; it consists of calculating the radius between circular–circular interpolations in relation to the tolerance ε imposed on the designed piece.

2.1 Feed rate modeling

Circular interpolation is a mode of work used in manufacturing. This mode is greatly dependent on kinematic performances of the machine [8] and on the physical phenomenon of cutting [14, 15].

2.1.1 Analytical feed rate modeling

In this part, a kinematic behavior study of a machine tool following a circular path in the plane (XY) is proposed (Fig. 2). The equation of curvilinear movement law during a circular profile is

CC': acceleration length L_{acc}
 C'D': tool path followed with V_m
 D'D: deceleration length L_{dec}

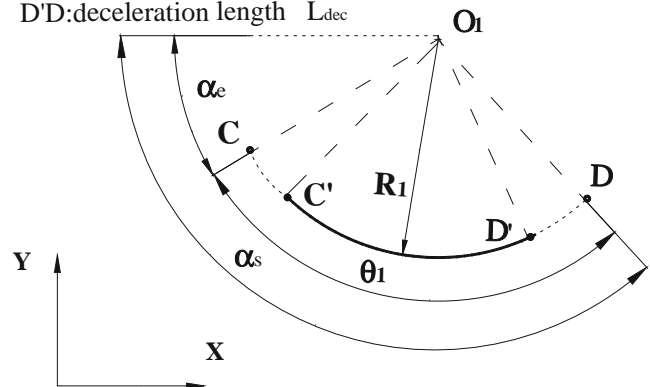
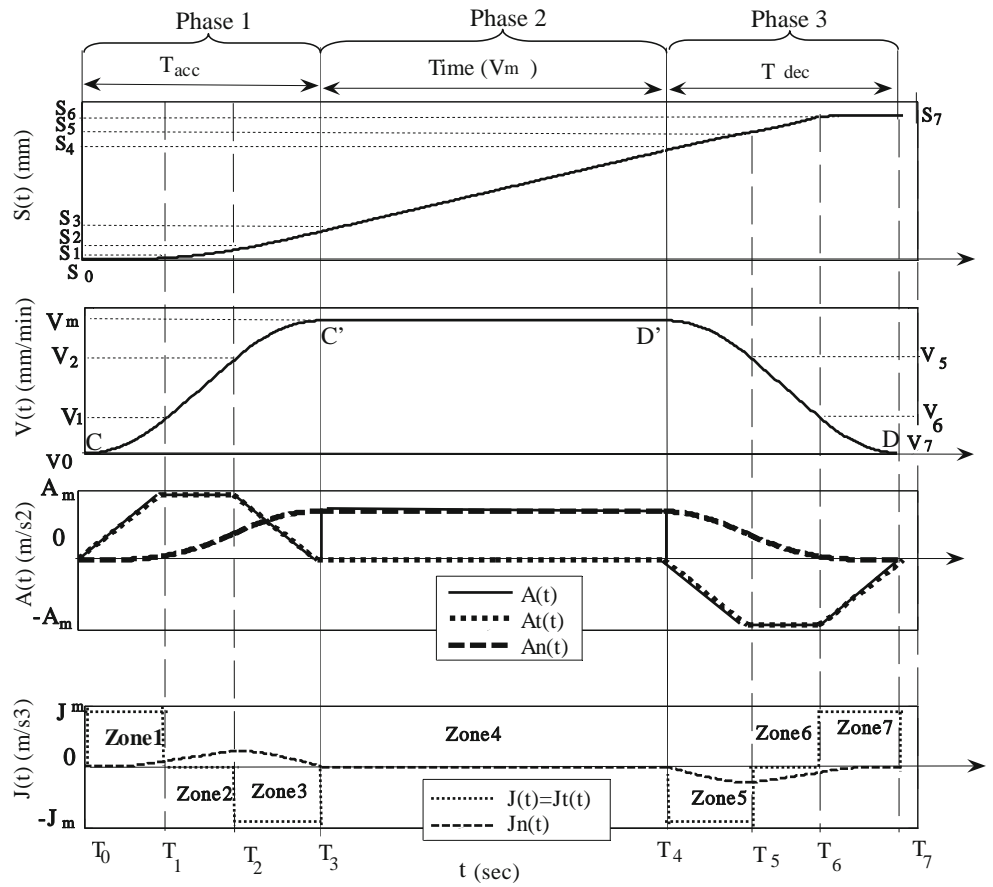


Fig. 2 Circular interpolation

Fig. 3 Kinematic profiles for constant jerk-based feed rate generation



$$\vec{V} = \frac{ds(t)}{dt} \vec{T} = V(t) \vec{T} \quad (1)$$

$$\vec{J}_R = \frac{d\vec{A}}{dt} = \frac{dA_t}{dt} \vec{T} + \frac{dA_n}{dt} \vec{N} = \frac{dV^2(t)}{dt^2} \vec{T} + 2 \frac{V(t)}{R_1} \frac{dV(t)}{dt} \vec{N} = J_t(t) \vec{T} + J_n(t) \vec{N} \quad (3)$$

$$\vec{A}_R = \frac{d\vec{V}}{dt} = \frac{dV(t)}{dt} \vec{T} + \frac{V^2(t)}{R_1} \frac{d\vec{T}}{dt} = A_t(t) \vec{T} + A_n(t) \vec{N}$$

(2)

with $A_t(t) = \frac{dV(t)}{dt}$ $A_n(t) = \frac{V^2(t)}{R_1}$

with $J_t(t) = \frac{dV^2(t)}{dt^2}$ $J_n(t) = 2 \frac{V(t)}{R} \frac{dV(t)}{dt}$ \vec{A}_R and \vec{J}_R are respectively the resultant vector of acceleration and jerk. In a circular interpolation, the acceleration has two components: tangential acceleration $A_t(t)$ and a normal

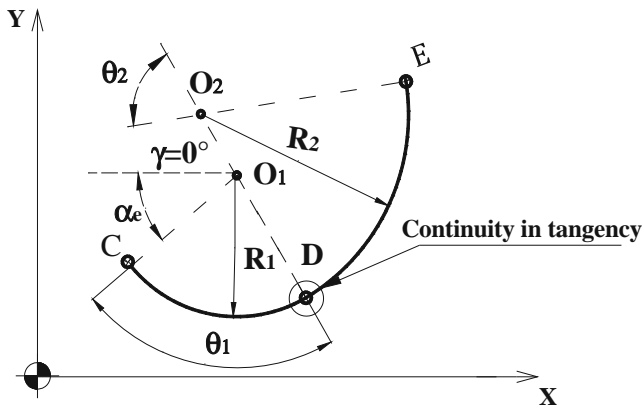


Fig. 4 Programmed tool path; $\gamma=0^\circ$

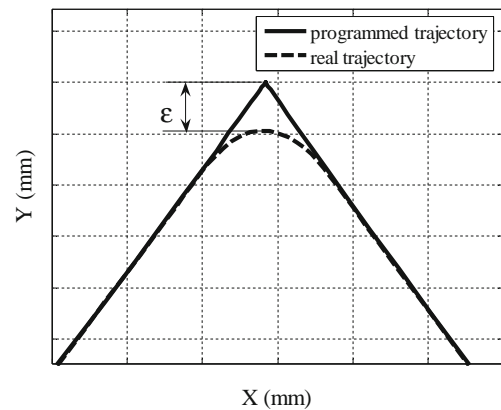
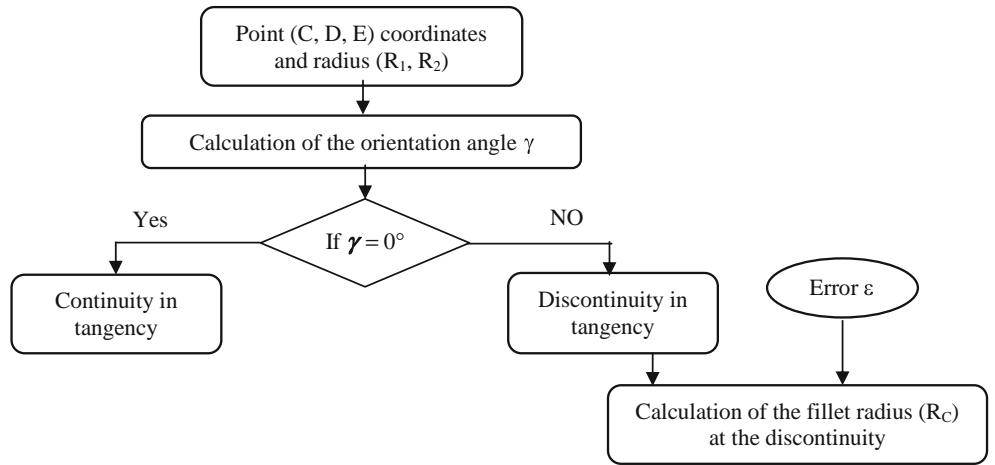


Fig. 5 Programmed and real trajectory

Fig. 6 Recursive algorithm for geometric modeling of tangency discontinuity



acceleration $A_n(t)$. Each component of acceleration is controlled by a tangential jerk $J_t(t)$ and a normal jerk $J_n(t)$. For acceleration and deceleration phases, tangential jerk has a step profile; however, normal jerk has variable and low value (as shown on Fig. 1). For all other phases, tangential and normal jerks are null. In addition to that, the machine axes are driven by a constant value of the jerk. So, in this work only tangential jerk is considered.

Pateloup [4] and Erkorkmaz [15] have developed an analytical modeling of the feed rate for a linear interpolation. Based on these works, the analytical feed rate modeling is transposed for circular interpolation. New equations given by this transposition are detailed as following.

For motion along the tool path, the value of jerk is constant, so the acceleration has trapezoidal profiles.

Zone 1: The acceleration has linear profiles, the feed rate has parabolic profiles and the displacement has cubic profiles.

S_0 is the length of the last block, $S_i = S(T_i)$ and $V_i = V(T_i)$ with $i=0$ to 7.

$$\forall t \in [T_0, T_1] \left\{ \begin{array}{l} J_1(t) = J_{t1}(t) = J_m J_{t1}(t) = \frac{dV_1^2(t)}{dt^2} \quad J_{n1}(t) = 2 \frac{V_1(t)}{R_1} \frac{dV_1(t)}{dt} \\ A_1(t) = A_{t1}(t) = J_m t \quad A_{n1}(t) = \frac{dV_1(t)}{dt} \quad A_{n1}(t) = \frac{V_1^2(t)}{R_1} \\ V_1(t) = \frac{J_m}{2} t^2 + V_0 \\ S_1(t) = \frac{J_m}{6} t^3 + V_0 t + S_0 \end{array} \right.$$

Zone 2: The feed rate has linear profiles, the acceleration values are constant, and the Jerk of work is 0.

$$\forall t \in [T_1, T_2] \left\{ \begin{array}{l} J_2(t) = J_{t2}(t) = 0 \quad J_{n2}(t) = 0 \quad J_{n2}(t) = 2 \frac{V_2(t)}{R_1} \frac{dV_2(t)}{dt} \\ A_2(t) = A_{t2}(t) = J_m T_1 = A_m \quad A_{n2}(t) = \frac{dV_2(t)}{dt} \quad A_{n2}(t) = \frac{V_2^2(t)}{R_1} \\ V_2(t) = J_m T_1 (t - T_1) + V_1 \\ S_2(t) = \frac{J_m T_1}{2} (t - T_1)^2 + V_1 (t - T_1) + S_1 \end{array} \right.$$

Fig. 7 Fillet radius between circular-circular contour

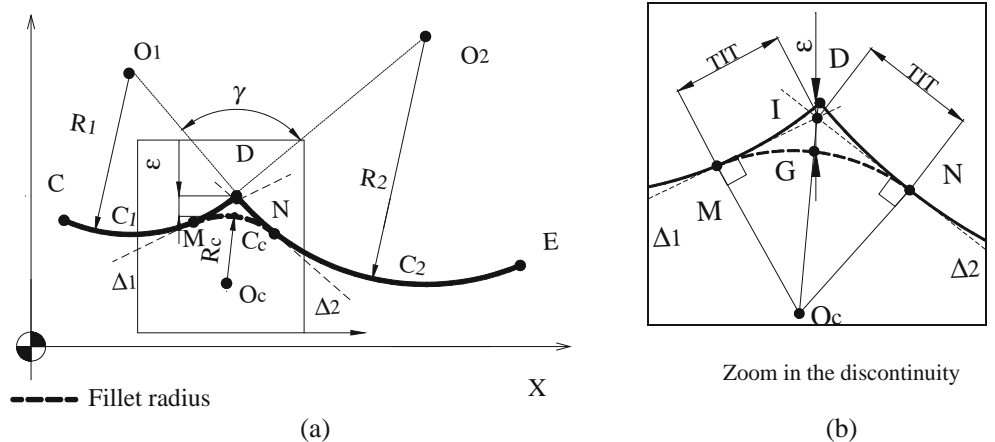


Table 1 Geometric parameters of the tool path ($\theta_1 = \theta_2 = 80^\circ$)

		$\varepsilon=0.2$ mm					γ ($^\circ$)	Type of discontinuity	R_c (mm)	TIT (mm)
		Points coordinates								
		C	D	E	R_1	R_2				
Case1	X	10	61.42	74.81	40	60	0	In curvature	-	-
	Y	20	20	95.96	40	60				
Case2	X	10	46.36	109.54	40	60	90	In tangency	0.49	0.48
	Y	20	56.36	100.6	40	60				
Case3	X	10	61.42	120.51	40	60	120	In tangency	0.205	0.35
	Y	20	20	-29.58	40	60				

Zone 3: The profiles generated looks like the profiles of zone 1.

$$\forall t \in [T_2, T_3] \left\{ \begin{array}{l} J_3(t) = J_{t3}(t) = -J_m J_{t3}(t) = \frac{dV_3^2(t)}{dt^2} \quad J_{n3}(t) = 2 \frac{V_3(t)}{R_1} \frac{dV_3(t)}{dt} \\ A_3(t) = A_{t3}(t) = -J_m(t - T_2) + J_m T_1 \quad A_{t3}(t) = \frac{dV_3(t)}{dt} \quad A_{n3}(t) = \frac{V_3^2(t)}{R_1} \\ V_3(t) = -\frac{J_m}{2}(t - T_2)^2 + J_m T_1(t - T_2) + V_2 \\ S_3(t) = -\frac{J_m}{6}(t - T_2)^3 + \frac{J_m T_1}{2}(t - T_2)^2 + V_2(t - T_2) + S_2 \end{array} \right.$$

Zone 4: It corresponds to a feed rate equal to the maximum value and zero acceleration and jerk.

$$\forall t \in [T_3, T_4] \left\{ \begin{array}{l} J_4(t) = J_{t4}(t) = 0 \quad J_{t4}(t) = 0 \quad J_{n4}(t) = 0 \\ A_4(t) = A_{n4}(t) = \frac{V_m^2}{R_1} \quad A_{t4}(t) = 0 \quad A_{n4}(t) = \frac{V_m^2}{R_1} \\ V_4(t) = V_3 = V_m \\ S_4(t) = V_m(t - T_3) + S_3 \end{array} \right.$$

Zone 6: The profiles generated looks like the profiles of zone 2.

$$\forall t \in [T_5, T_6] \left\{ \begin{array}{l} J_6(t) = J_{t6}(t) = 0 \quad J_{t6}(t) = 0 \quad J_{n6}(t) = 2 \frac{V_6(t)}{R_1} \frac{dV_6(t)}{dt} \\ A_6(t) = A_{t6}(t) = -J_m(T_5 - T_4) = -A_m \quad A_{t6}(t) = \frac{dV_6(t)}{dt} \quad A_{n6}(t) = \frac{V_6^2(t)}{R_1} \\ V_6(t) = -J_m(T_5 - T_4)(t - T_5) + V_5 \\ S_6(t) = \frac{-J_m(T_5 - T_4)}{2}(t - T_5)^2 + V_5(t - T_5) + S_5 \end{array} \right.$$

Zone 5: The profiles generated looks like the profiles of zone 1.

$$\forall t \in [T_4, T_5] \left\{ \begin{array}{l} J_5(t) = J_{t5}(t) = -J_m J_{t5}(t) = \frac{dV_5^2(t)}{dt^2} \quad J_{n5}(t) = 2 \frac{V_5(t)}{R_1} \frac{dV_5(t)}{dt} \\ A_5(t) = A_{t5}(t) = -J_m(t - T_4) \quad A_{t5}(t) = \frac{dV_5(t)}{dt} \quad A_{n5}(t) = \frac{V_5^2(t)}{R_1} \\ V_5(t) = -\frac{J_m}{2}(t - T_4)^2 + V_m \\ S_5(t) = -\frac{J_m}{6}(t - T_4)^3 + V_m(t - T_4) + S_4 \end{array} \right.$$

Zone 7: The profiles generated looks like the profiles of zone 1.

$$\forall t \in [T_6, T_7] \left\{ \begin{array}{l} J_7(t) = J_{t7}(t) = J_m J_{t7}(t) = \frac{dV_7^2(t)}{dt^2} \quad J_{n7}(t) = 2 \frac{V_7(t)}{R_1} \frac{dV_7(t)}{dt} \\ A_7(t) = A_{t7}(t) = J_m(t - T_6) - J_m(T_5 - T_4) \quad A_{t7}(t) = \frac{dV_7(t)}{dt} \quad A_{n7}(t) = \frac{V_7^2(t)}{R_1} \\ V_7(t) = \frac{J_m}{2}(t - T_6)^2 - J_m(T_5 - T_4)(t - T_6) + V_6 \\ S_7(t) = \frac{J_m}{6}(t - T_6)^3 - J_m(T_5 - T_4)(t - T_6)^2 + V_6(t - T_6) + S_6 \end{array} \right.$$

The limit conditions of the feed rate are

The input parameters,
 $V_0, V_7, A_m, J_m, \theta_1, R_1,$
and V_m

T_i	V_i	S_i
T_0	V_0	S_0
T_1	$V_1 = \frac{J_m}{2} T_1^2 + V_0$	$S_1 = \frac{J_m}{6} T_1^3 + V_0 T_1 + S_0$
T_2	$V_2 = J_m T_1 (T_2 - \frac{T_1}{2}) + V_0$	$S_2 = \frac{J_m T_1^3}{6} + \frac{J_m}{2} T_1 T_2 (T_2 - T_1) + V_0 T_2 + S_0$
T_3	$V_3 = J_m T_1 T_2 + V_0 = V_m$	$S_3 = \frac{J_m T_1 T_2}{2} (T_2 + T_1) + V_0 T_3 + S_0$
T_4	$V_4 = V_m$	$S_4 = V_m (T_4 - T_3) + S_3$
T_5	$V_5 = -\frac{J_m}{2} (T_5 - T_4)^2 + V_m$	$S_5 = -\frac{J_m}{6} (T_5 - T_4)^3 + V_m (T_5 - T_4) + S_3$
T_6	$V_6 = -\frac{J_m}{2} (T_5 - T_4)(2T_6 - T_5 - T_4) + V_m$	$S_6 = -\frac{J_m (T_5 - T_4)^3}{6} + \frac{J_m}{2} (T_5 - T_4)(T_6 - T_5)$ $(T_6 - T_4) + V_m (T_6 - T_3) + S_3$
T_7	$V_7 = -J_m (T_5 - T_4)(T_6 - T_4) + V_m$	$S_7 = -\frac{J_m (T_5 - T_4)(T_6 - T_4)}{2} (T_6 + T_5 - 2T_4)$ $+ V_m (T_7 - T_3) + S_3 = \theta_1 R_1$

The duration of each phase T_i (T_1 to T_7) is calculated according to the geometric and kinematic constraints using modeling results. MATLAB© software is used in order to develop a feed rate simulator. The kinematic profiles used in feed rate generation are showed on Fig. 3.

For a circular interpolation, the movement law of feed rate is divided into three phases. As depicted on Fig. 3, during the first phase (CC'), the feed rate increases and reaches the stationary value, and the tangential acceleration increases until reaching its maximum value then decrease until it vanishes. This is generated on the basis of the

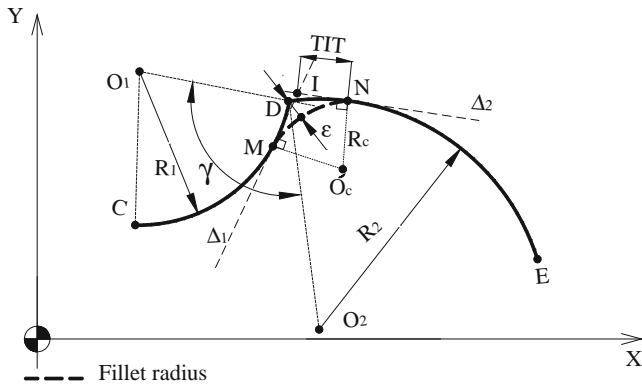


Fig. 8 Fillet radius between circular-circular contour

minimal tangential jerk achievable in the circle. In this phase, the jerk of work is equal to tangential jerk. In the second phase (C'D'), the maximal feed rate was achieved, the corresponding acceleration is only normal, and the normal jerk J_n is null. It can be concluded that during circular interpolation, the tangential jerk value is controlled by the numerical control unit (NCU) in order to generate a feed rate limited by the maximum axis jerk [8]. Finally, the third phase (D'D) is totally symmetric to the first phase.

2.1.2 Different types of feed rate limitation in circular interpolation

1. Constraint imposed by the capacities of the axes

The less dynamic axis requires its capabilities during kinematic displacement when interpolated between several axes. The optimum solution is to use an axis to its maximum capacity or to define the following limitation [8]:

$$\begin{aligned}
 v_1 &= \min \left(\frac{V_{mX}}{|\cos \alpha_p|}, \frac{V_{mY}}{|\sin \alpha_p|} \right); A_m \\
 &= \min \left(\frac{A_{mX}}{|\cos \alpha_e|}, \frac{A_{mY}}{|\sin \alpha_e|} \right); J_m \\
 &= \min \left(\frac{J_{mX}}{|\cos \alpha_p|}, \frac{J_{mY}}{|\sin \alpha_p|} \right)
 \end{aligned}$$

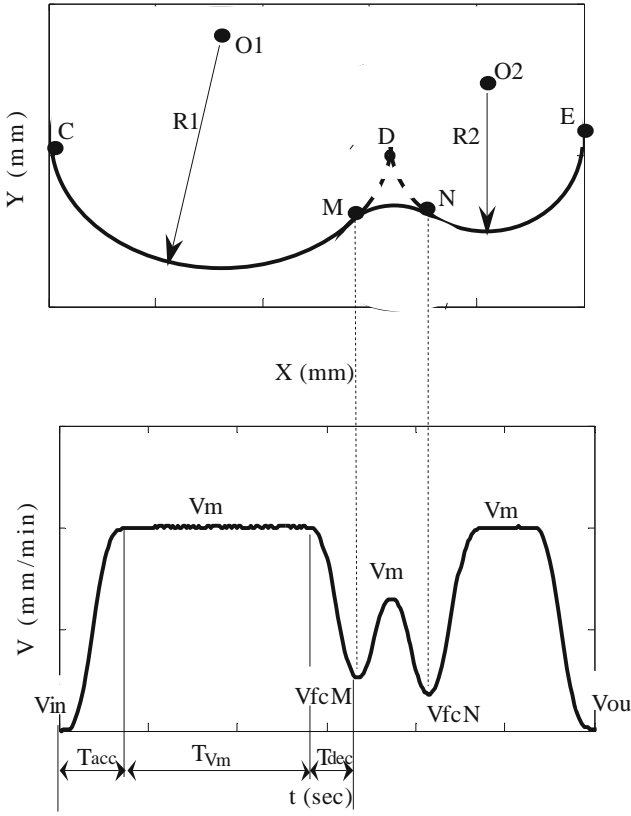


Fig. 9 Feed rate profile for the circular-circular contour

With $\alpha_p \in [\alpha_e, \alpha_s]$; $\alpha_s - \alpha_e = \theta$ and $\alpha_e = \arccos\left(\frac{|X_{O1} - X_C|}{R_1}\right)$

α_p , α_e , α_s , V_l , V_{mX} , V_{mY} , A_{mX} , A_{mY} , J_{mX} , and J_{mY} are respectively the angular position, the input angle, the output angle, the attainable feed rate according to axis feed rate capacity, the maximum feed rate for the X -axis, the maximum feed rate for the Y -axis, the maximum acceleration for the X -axis, the maximum acceleration for the Y -axis, the maximum jerk for the X -axis, and the maximum jerk for the Y -axis. When the stationary feed rate is reached, the two corresponding parameters are normal acceleration $A_n = A_m$ and tangential jerk $J_t = J_m$.

When we use the limitation of the normal acceleration, the feed rate is [6]

$$V_{An} = \sqrt{R_1 A_n} \quad (4)$$

When we use the limitation of the tangential jerk, the feed rate is deduced from Eq. 3 [6]:

$$V_{Jt} = \sqrt[3]{J_t R_1^2} \quad (5)$$

2. Constraint imposed by NCU

For small radius values, the feed rate will be limited by the NCU. The feed rate $V_{t_{cy}}$ limited by the interpolation cycle time t_{cy} is

$$V_{t_{cy}} = \frac{R_1 \theta_1}{t_{cy}} = \frac{L_b}{t_{cy}} \quad (6)$$

with L_b as the total length of the block.

3. Constraint imposed by the tool path length

In this case, the sum of the acceleration and deceleration length (L_{acc} and L_{dec}) is superior to L_b . So, the machine never finds the sufficient stroke to reach the maximum feed rate. The feed rate V_{L_b} limited by the length of the tool path is calculated by using the analytical model presented in the beginning.

4. Conclusion

The feed rate V_m is related to three types of parameters: adjustments and capacity of NCU ($V_{t_{cy}}$), the NC programs (V_{prog} ; V_{L_b}), and the capacities of the axes (V_I ; V_{An} ; V_{Jt})

Feed rate for the circular interpolation is $V_m = \min(V_I; V_{prog}; V_{Jt}; V_{An}; V_{t_{cy}}; V_{L_b})$.

2.2 Transition feed rate modeling

At the time of a discontinuity in tangency or in curvature, numerical control unit slows down in order to respect the maximum values of acceleration and jerk for each axis. In the crossing of a discontinuity in curvature $\gamma=0^\circ$ (continuity in tangency) (point D) (Fig. 4), the transition feed rate V_{fc} has to be equal to 0 and the second derivatives of the tangent to the tool path $\frac{d^2(T)}{ds^2}$ is not defined.

The feed rate for a discontinuity in curvature between two circle arcs with different radius values is proposed in [12]:

$$V_{fc} = \sqrt{\frac{R_1 R_2 J_m \delta t}{|R_1 - R_2|}} \quad (7)$$

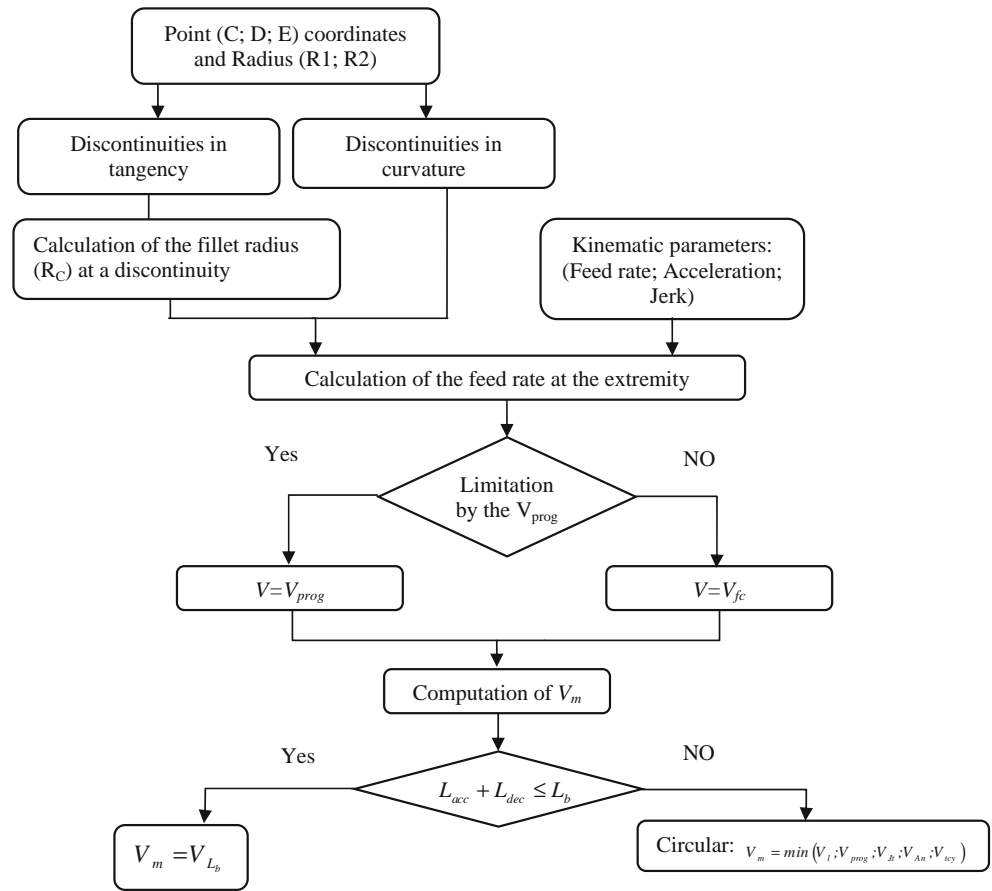
The value of jerk J_m in the point D is

$$J_m = \min\left(\frac{J_{mX}}{|\cos(\alpha_e + \theta_1)|}, \frac{J_{mY}}{|\sin(\alpha_e + \theta_1)|}\right)$$

In the crossing of a discontinuity in tangency $\gamma \neq 0^\circ$, two methods will be considered. The first is to annul the feed rate on this discontinuity. This implied a stop of cutting process, brand of the part, and an increase in the cycle time.

The second method is to authorize an error (ε) between the programmed trajectory and the real trajectory to obtain a non-null feed rate of transition (Fig. 5). In this case, the tool

Fig. 10 Recursive algorithm for estimating the feed rate



does not pass along the point of discontinuity. This will be detailed in the following part.

2.3 Geometric modeling of tangency discontinuity

In this part, a geometrical model of t.d. is presented (as shown on Fig. 1). For the modeling, the considered trajectory of tool center is generated by CAM software. The method of the tangency discontinuity modeling between two circular interpolations is detailed on Fig. 6.



Fig. 11 Machining center Huron KX10

2.3.1 Influence of tool path geometry on the type of discontinuity

For the machining operation, there was a discontinuity in curvature or in tangency on the level of direction shift; this makes the movement slow down. This type of this

Table 2 Machine characteristics

Huron KX10	
Spindle	
Spindle speed	100–24,000 rev/min
Maximum power	20 kW
Axis capacity	
Maximum fast speed XY	30 m/min
Maximum fast speed Z	18 m/min
Feed rate XY	10 m/min
Maximum acceleration XY	3 m/s ²
Maximum jerk XY	50 m/s ³
NCU	
Design	Siemens 840D
Acceleration mode	Soft
the tangential displacement mode	G64 and G641
Look ahead	100 blocks
Interpolation cycle time t_{cy}	2 ms

discontinuity depends on the orientation angle γ (as shown on Fig. 1).

The angle γ has the following form:

$$\gamma = \frac{\theta_1}{2} + \frac{\theta_2}{2} + \alpha - \beta \quad (8)$$

From Eq. 8, two cases of the discontinuity are distinguished:

- Curvature discontinuity (continuity in tangency) $\gamma=0^\circ$.
- Tangency discontinuity $0^\circ < \gamma < 180^\circ$.

The orientation angle γ has a great influence on the type of discontinuity and the feed rate evolution. It is determined from the points C , D , and E coordinates using a geometry equations (Eqs. 8, 9 and 10).

In the following part, a fillet radius modeling is developed in two steps. The first step permits to calculate the angle γ basing on the points C , D , and E coordinates. The second step consists of modeling the fillet radius value between circular–circular interpolation in relation to the tolerance ε imposed on the piece design.

2.3.2 Fillet radius modeling

The modeling of the fillet radius can be presented by two methods. In the first, the fillet radius between the two arcs is defined with NC function of the tangential displacement mode (G641) of Sinumerik language [3]. The value of the fillet radius depends on the distance TIT¹ (as shown on Fig. 7) which is the tolerance of interpolation of the trajectory. The distance must be specified with ADIS (circle arc inserted by NCU). In the second method, the fillet radius between the two arcs can be defined with a modal instruction RNDM or a not modal instruction RND² (circle arc inserted in NC programs).

As said before, the machine slowed down on the level of discontinuities in tangency. So, the control unit allows a non-null feed rate if an error ε is defined. This creates an arc of a circle (radius R_c) which depends on imposed error ε on orientation.

In the case of circular–circular interpolation (as shown on Fig. 1), the tool path is represented by two arcs: (CD; circle C_1 , radius R_1 , and center O_1) and (DE; circle C_2 , radius R_2 , and center O_2).

The coordinates of point E are given by:

$$\begin{aligned} X_E &= 2R_2 \sin \frac{\theta_2}{2} \cos \beta + X_D \\ Y_E &= 2R_2 \sin \frac{\theta_2}{2} \sin \beta + Y_D \end{aligned} \quad (9)$$

Where X_D and Y_D are the point D coordinates, they are given by:

$$\begin{aligned} X_D &= 2R_1 \sin \frac{\theta_1}{2} \cos \alpha + X_C \\ Y_D &= 2R_1 \sin \frac{\theta_1}{2} \sin \alpha + Y_C \end{aligned} \quad (10)$$

Where X_C and Y_C are the point C coordinates

1. Concave–concave contour

Figure 7a shows a path with a discontinuity in tangency located at connection between two concave circular contours with the angle of orientation $\gamma > 0^\circ$. In this case, the two centers $O_1 (X_{O1}, Y_{O1})$ and $O_2 (X_{O2}, Y_{O2})$ are placed on the same side of the trajectory.

Firstly, the angles θ_1 , θ_2 , β , and α are determined using Eqs. 9 and 10 and then the angle γ is calculated from the Eq. 8.

The fillet radius, which depends on the imposed error ε (Fig. 7b), is given by:

$$\varepsilon = \sqrt{(X_D - X_G)^2 + (Y_D - Y_G)^2} \quad (11)$$

The equation of the circular interpolation in arc CD is

$$(X - X_{O1})^2 + (Y - Y_{O1})^2 = R_1^2 \quad (12)$$

The equation of the circular interpolation in arc DE is

$$(X - X_{O2})^2 + (Y - Y_{O2})^2 = R_2^2 \quad (13)$$

The coordinates of the point O_c and the radius R_c are calculated by:

$$\begin{cases} (X_{O_c} - X_{O1})^2 + (Y_{O_c} - Y_{O1})^2 = (R_1 + R_c)^2 \\ (X_{O_c} - X_{O2})^2 + (Y_{O_c} - Y_{O2})^2 = (R_2 + R_c)^2 \\ (X_{O_c} - X_D)^2 + (Y_{O_c} - Y_D)^2 = (\varepsilon + R_c)^2 \end{cases}$$

TIT is calculated in relation to ε . It is introduced to the zone from which or to which the block transition is rounded (as shown on Fig. 7b) when TIT = IM = IN.

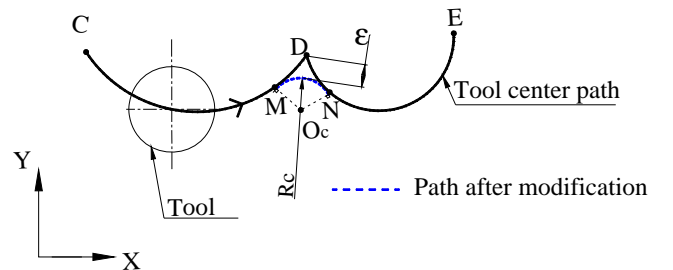


Fig. 12 Tool path geometry

¹ The distance which the rounding block may begin.

² Instruction of rounding the corner of the contour of Sinumerik language: RNDM, model instruction; RND, not model instruction

Table 3 Geometric parameters

Discontinuity in D															
	Points coordinates			R_1 (mm)	R_2 (mm)	θ_1 (°)	θ_2 (°)	γ (°)	Type of discontinuity	ε (mm)	R_c (mm)	TIT (mm)	V_{prog} (mm/ min)		
	C	D	E												
Test 1	X	10	67.85	143.81	40	60	80	80	90	In tangency	Case1	0.213	0.51	–	10,000
	Y	20	20	6.6							Case2	0.213	0.51	0.5	1,000
											Case3	2.24	8	–	10,000
Test 2	X	10	61.42	74.81	40	60	80	80	0	In curvature	–	–	–	10,000	
	Y	20	20	95.96											

With I as the intersection between Δ_1 and Δ_2 , Δ_1 is the tangent to the circle C_1 at point M , and Δ_2 is the tangent to the circle C_2 at point N .

The point M belongs to circles C_c and C_1 and N belongs to circles C_c and C_2 . Thus the coordinates of N and M are calculated using the circle equations.

The coordinates of point I may be calculated by:

$$\begin{cases} (X_M - X_I)^2 + (Y_M - Y_I)^2 = (X_N - X_I)^2 + (Y_N - Y_I)^2 \\ -\frac{X_{O_1} - X_M}{Y_{O_1} - Y_M} X_I - Y_I + \frac{X_{O_1} X_M + Y_{O_1} Y_M - X_M^2 - Y_M^2}{Y_{O_1} - Y_M} = 0 \end{cases} \quad (14)$$

The value of (TIT) is given by:

$$TIT = \sqrt{(X_M - X_I)^2 + (Y_M - Y_I)^2} \quad (15)$$

Table 1 presents an application of the model developed for three different geometries of the trajectory shown on Fig. 7 for an imposed error ε equal to 0.2 mm. The first case corresponds to an angle γ equal to 0; the second and the third cases correspond to angle γ values different from 0.

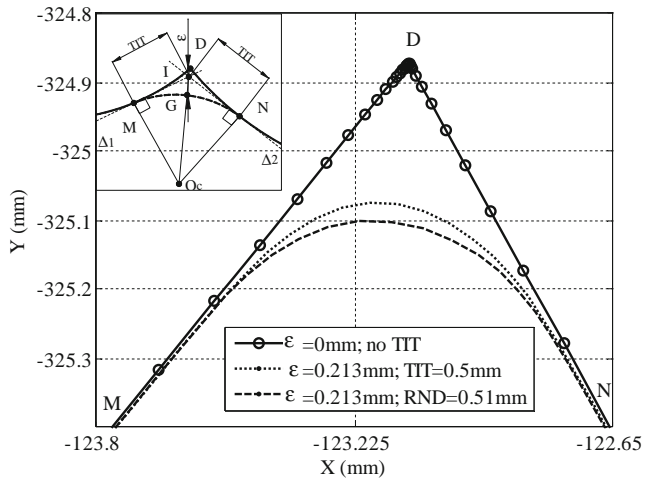


Fig. 13 Insertion of a circle arc which crosses discontinuity in tangency by G641 and RND function

In the last cases, it is noted that the angle γ has a great influence on the value of the fillet radius R_c .

2. Concave–convex contour

Figure 8 shows a fillet radius between concave circular and convex circular interpolation. In this case, the two centers O_1 and O_2 were placed on different sides on the trajectory.

R_c , X_{O_c} , and Y_{O_c} are calculated as follows:

$$\begin{cases} (X_{O_c} - X_{O_1})^2 + (Y_{O_c} - Y_{O_1})^2 = (R_1 + R_c)^2 \\ (X_{O_c} - X_{O_2})^2 + (Y_{O_c} - Y_{O_2})^2 = (R_2 - R_c)^2 \\ (X_{O_c} - X_D)^2 + (Y_{O_c} - Y_D)^2 = (\varepsilon + R_c)^2 \end{cases}$$

In Siemens NCU, the TIT value must not exceed 0.5 mm. If it is the case, the radius R_c must be introduced in the program with circular interpolation (G02 and G03) between M and N or by a modal instruction RNDM or a not modal instruction RND.

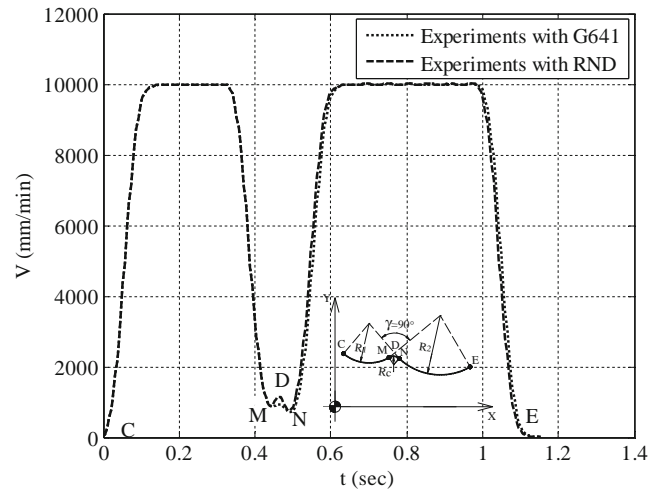


Fig. 14 Experimental variation of feed rate for the RND and G641 function

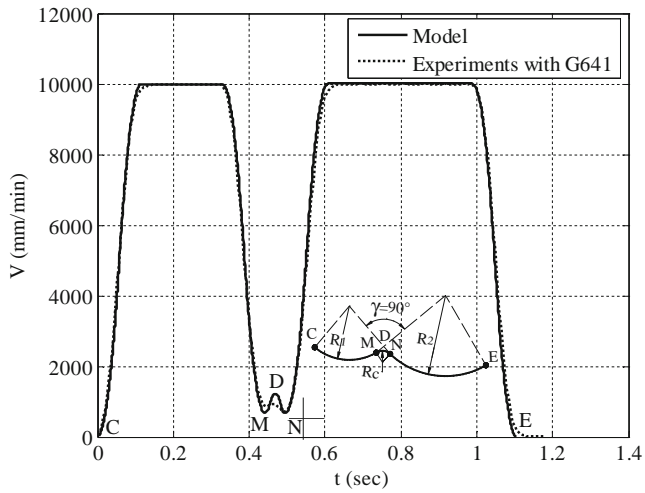


Fig. 15 Theoretical and experimental variation of feed rate; TIT=0.5

2.3.3 Methodologies of feed rate calculation in the crossing of a continuity in tangency

In this part, the methodology of calculating the feed rate at crossing in two circular interpolations is detailed. A discontinuity in tangency is located between these two interpolations at point *D*. This discontinuity is eliminated by the insertion of arc *MN*.

Figure 9 depicts the correspondence between the tool path and the feed rate profile. The modeling steps are represented in the following diagram shown on Fig. 10:

The modeling steps are as follows:

- Determination of the angle γ using the point coordinates to identify the type of discontinuity using Eq. 8.
- Calculation of the fillet radius (R_C), if it is a discontinuity in tangency.
- Calculation of the feed rate at the extremity using Eq. 7.

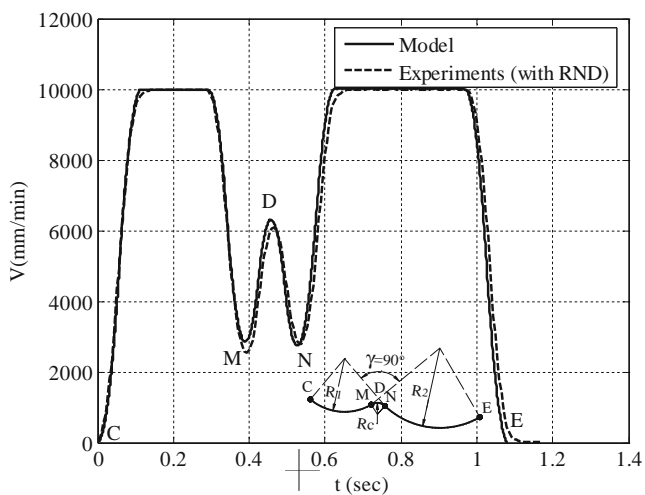


Fig. 16 Theoretical and experimental variation of feed rate

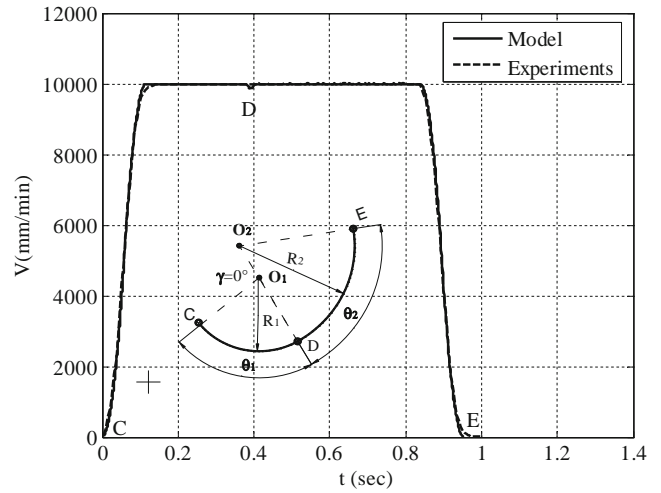


Fig. 17 Theoretical and experimental variation of feed rate

- Computation of the maximum feed rate $V_m = \min(V_1; V_{prog}; V_{Jt}; V_{An}; V_{tcy}; V_{Lb})$.
- Calculation of the duration of each phase T_i (T_1 to T_7) for each block.
- Plot the evolution of feed rate in function of time using MATLAB© software.

3 Experimental tests and results

3.1 Experimental method

In order to validate the models and to determine the influence of the geometry of the trajectory on the feed rate evolution and the fillet radius, experiments were carried out on a high-speed machine (as shown on Fig. 11). See machine characteristics in Table 2.

The HSM configuration adopted for this experimental study integrates the continuous path mode with the tangential displacement mode (G641) and the “soft” acceleration mode [4]. In order to determine the influence of the geometry of the trajectory on the feed rate evolution and to validate the developed model, the tool path presented on Fig. 12 and following several tests was designed (see Table 3) afterwards an industrial application was carried out.

Based on a geometry presented in test 1 (as shown on Table 3), Fig. 13 shows a comparison between the

Table 4 Fillet radius in relation to error

The geometric parameters is presented in test 1 (Table 3)

ε (mm)	0.02	0.08	0.213	0.41	0.68	1.29	1.84	2.24	4.09
R_c (mm)	0.05	0.22	0.51	1.2	2	4	6	8	15
TIT (mm)	0.05	0.2	0.5	-	-	-	-	-	-

transition trajectory generated by G641 and RND function (case1 and case2). In experimental study, the real tool path is registered.

For the same error value ($\varepsilon=0.213$ mm), the tool path generated by the Siemens CNC (G641) at the transitions is slightly different from that generated with RND. In the first case, a polynomial trajectory interpolation can be used by the Siemens CNC, and this justifies the disparity between these results. This phenomenon is well met in the work of Pessoles [6] in the case of the transition between two linear interpolations.

Figure 14 shows not so great difference at the feed rate evolution between the two methods (with G641 and with RND). The difference between the transition trajectory generated by the RND and G641 function (as shown on Fig. 13) has no great impact on the cycle time. This is due to the small crossed distance during the block transition.

3.2 Results and discussion

3.2.1 Elementary tests

In order to validate the developed model and to determine the impact of the imposed error on the cycle time evolution, elementary tests are carried out. Based on a geometry presented in the test 1 (as shown on Table 3), the feed rate variation to crossing in the discontinuity in tangency is calculated (Fig. 15). Test 1 includes three cases studies. In the following, case 2 and case 3 are considered.

For the case 2, the discontinuity in tangency is eliminated by adding a circle arc which is a function of the TIT (as shown on Fig. 7). Case 3 is like the latter, although the circle arc is introduced in the program with RND function (Fig. 16).

Test 2 presents the geometrical parameters of a path with discontinuity in curvature ($\gamma=0^\circ$) located at connection between two circular contours. Figure 17 shows a feed rate variation to crossing in the discontinuity in curvature.

For the cases 2 and 3 (test 1), at discontinuity (point *D*), it is noted that the machine slows down immediately, only for test 2. For the circular interpolation, the machine adopted a maximum speed in relation to its capacities, type of discontinuity, and radius of trajectory.

The absence of acceleration and deceleration phases at the level of fillet radius in experimental graph (as shown on Fig. 15) was the result of experimental cycle time limitation of the machine. Indeed, the time of acceleration is inferior to experimental cycle time, which allows to conclude that the experimental cycle time is superior to theoretical cycle time ($t_{cy}=2$ ms).

So, the tool never finds the sufficient time to respect the theoretical variation of the feed rate. In order to define the impact of the error value on the cycle time, trajectories with

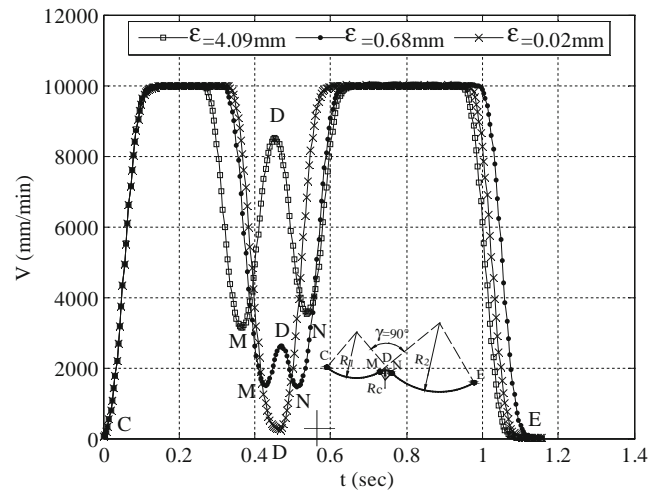


Fig. 18 Experimental variation of feed rate for various values of error (with RND function)

presenting two circular interpolations following several tests were designed (as shown on Table 4). These tests were developed in experimental and theoretical studies. The experimental study is obtainable in two methods. Firstly, the fillet radius between the two arcs is generated by NC function of the tangential displacement mode (G641) (if $TIT \leq 0.5$ mm). Secondly, the fillet radius is inserted in the NC programs with a circular interpolation (G02 and G03) or with a modal instruction RNDM or a not modal instruction RND.

Table 4 presents the fillet radius value in relation to error. Figures 18 and 19 show respectively the experimental feed rate evolution and the theoretical feed rate evolution for different values of the imposed error ε .

Figures 18 and 19 show a good correlation between the experimental and the theoretical results. It is noted that when

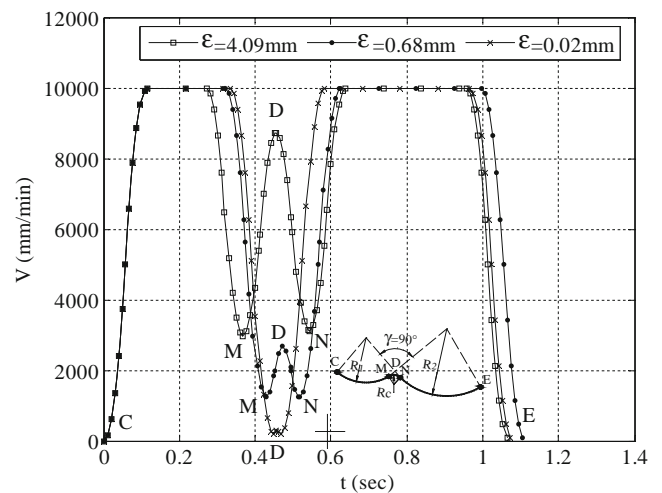
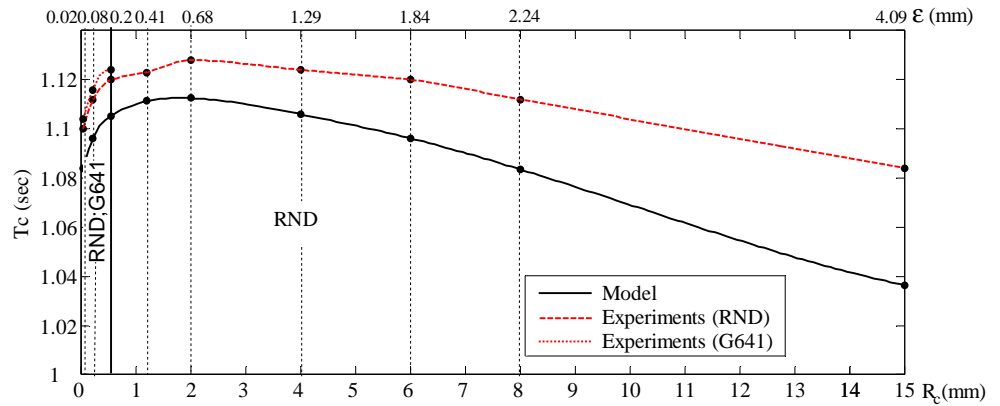


Fig. 19 Theoretical variation of feed rate for various values of error

Fig. 20 Impact of the error values on the cycle time



the error value increases, the fillet radius and the transition feed rate increases. However, this speed gain does not cause a decrease of the total cycle time. So, it is necessary to increase the fillet radius to find the optimal solution.

Figure 20 presents the evolution of the time function of the fillet radius and the values of the imposed error between the programmed and the real trajectory. It permits to define the fillet radius for a fixed value of the error ϵ .

Figure 20 illustrates that the maximum error between the theoretical and experimental results is 5 %. This error is almost constant for all tests. It represents a good estimation of the optimal fillet radius. It is proven that a small increase of the fillet radius value does not have a significant influence on the reduction of the cycle time. However, when the fillet radius value exceeds 2 mm, a reduction of cycle time can be obtained.

3.2.2 Industrial application

The proposed methodology for evaluating the feed rate was applied to a machined die of the SIAF Tunisian

manufacture (Fig. 21). The generated tool path includes the various cases of connection between two circular interpolations (Fig. 22c).

The final HSM configuration adopted for this application includes the continuous path mode smoothed by the tangential displacement mode (G641 with $TIT=0.05$ mm).

The tool path is generated with CAM software. The used machining strategy is contour parallel. The cutting parameters are the following: cutter tool diameter $d_{out}=20$ mm, programmed feed rate $V_{prog}=8,000$ mm/min, spindle speed $N=3,800$ rev/min, radial depth of cut $a_e=0.9d_{out}$, and axial depth of cut $a_p=0.3$ mm.

For this application, the feed rate variation is calculated during the sweeping of the first machining level as shown on Fig. 23. The proposed methodology for evaluating the feed rate in high-speed milling is based on the following elements:

- Generation of point coordinates of the trajectory (NCI file),

Fig. 21 Work piece configuration

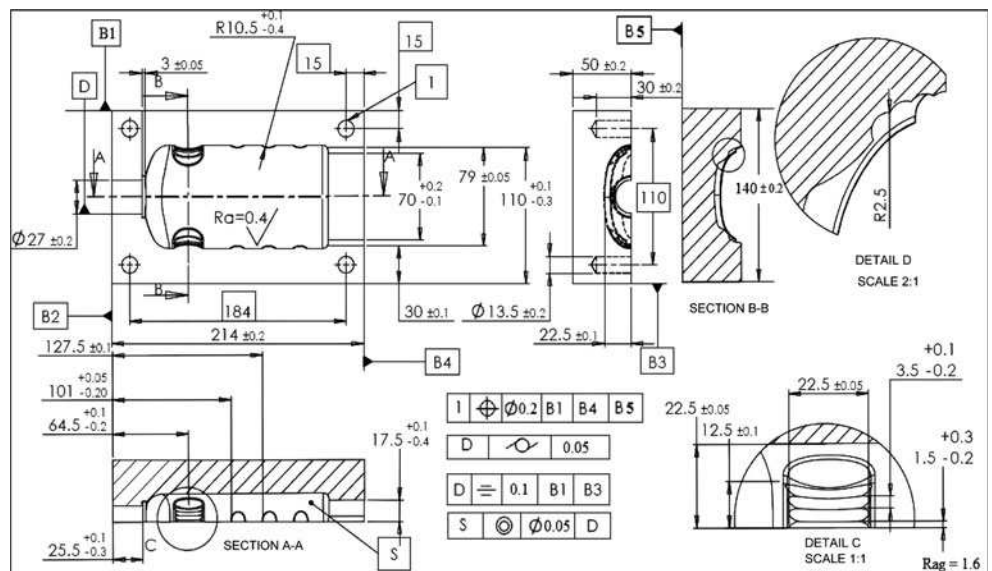
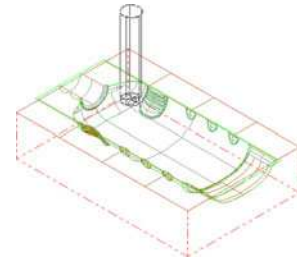


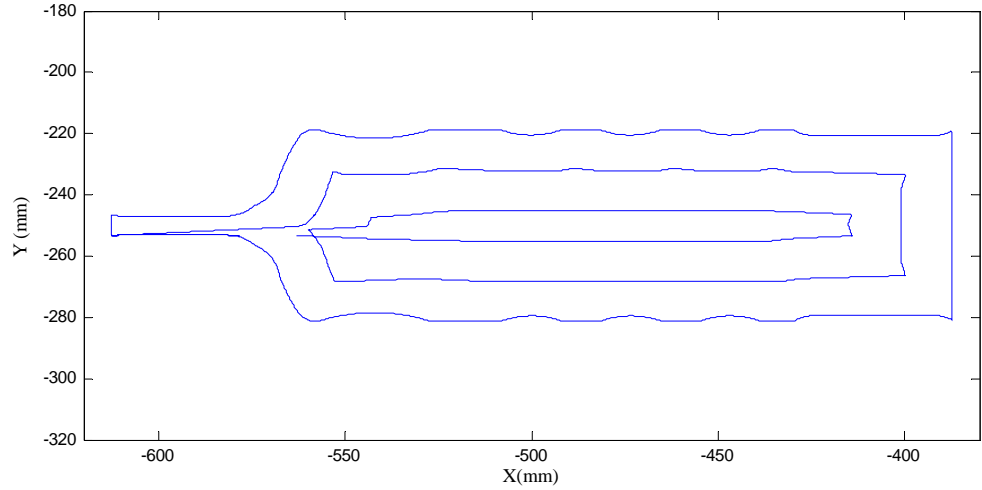
Fig. 22 Simulation and machining using a tool with a diameter of 20 mm



(a) Machining of the die



(b) Simulation on CAM Software



(c) Tool paths during the sweeping of the first machining level

- Modeling of the fillet radius at the discontinuities according to the imposed error, and
- Determination of the feed rate evolution and thereafter the cycle time under the kinematic constraints of the machine.

The percentage of the error between the theoretical and experimental values of the cycle time is 2 %. Figure 23 illustrates that the feed rate does not always reach the programmed value during the machining process.

For theoretical study, the percentage of the use of the programmed feed r_1 is calculated (as shown on Fig. 24). The percentage of the programmed of feed rate used is

$$r_1 = \frac{T_{V_{prog}}}{T_c} \quad (16)$$

The total time when we used the programmed feed rate $T_{V_{prog}}$ is determined according to the profile of the feed rate (as shown on Fig. 25). The total time $T_{V_{prog}}$ is given by

$$T_{V_{prog}} = \sum_i^{i=1} T_{V_{prog}} \quad (17)$$

It is noted that the percentage r_1 decreases by increasing the value of the programmed feed rate. Hence, it is

necessary to consider the variation of the feed rate in the calculation of cycle time.

The model used for this study allowed the estimation of the cycle time for the used machining strategy according to the imposed error and thereafter an estimation of the cycle time as a function of programmed feed rate (Fig. 26).

Figure 26 illustrates that the time T_{cCAM} calculated by CAM software (the trajectory length/programmed feed rate) is not representative of the real machining time. It can be concluded that the importance of this shift should be taken into account during the calculation of the time and the cost of machining.

For a programmed feed rate $V_{prog}=8,000$ mm/min, the total cycle time calculated by CAM software is given by:

$$T_{cCAM} = \frac{l_{tot}}{V_{prog}} = 9.76s \quad (18)$$

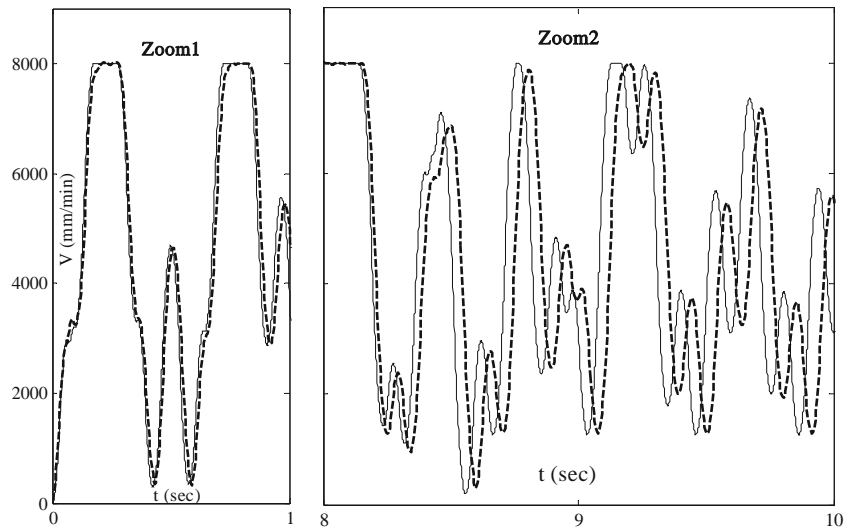
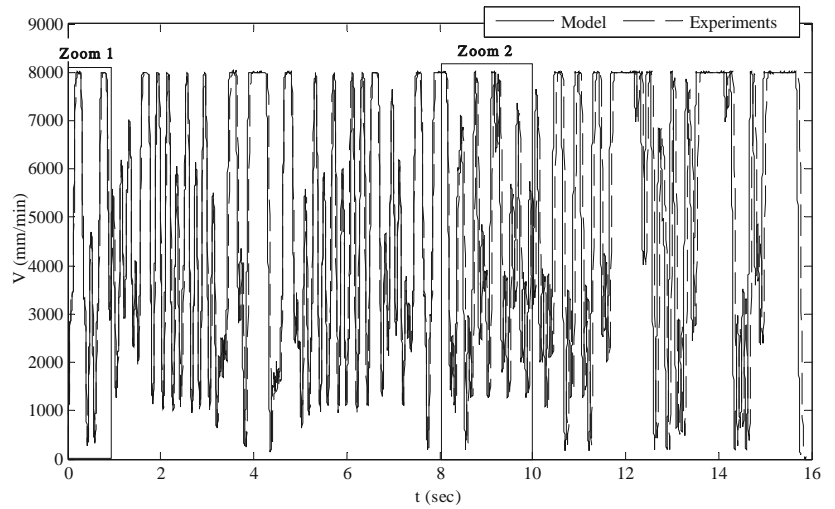
When we used a variable feed rate, the total cycle time is given by:

$$T_c = 15.77s$$

The report η showed that the estimated cost C_{est} is much higher than the actual cost C_{act} :

$$\eta = \frac{C_{act}}{C_{est}} = \frac{C_m T_c}{C_m T_c V_{prog}} = \frac{T_c}{T_c V_{prog}} 1.6 \quad (19)$$

Fig. 23 Theoretical and experimental variation of feed rate during the sweeping of the first machining level



C_{est} (estimated cost) is calculated as a function of the time T_{cCAM} calculated by CAM software. C_{act} (actual cost) is calculated as a function of the simulated time T_c .

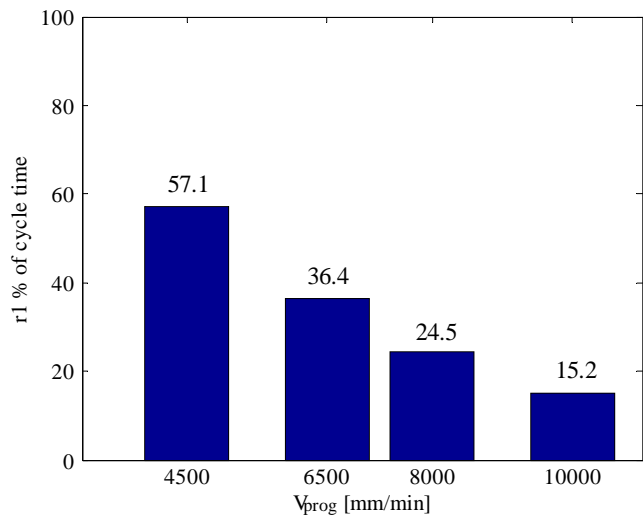


Fig. 24 Representative graph of using percentage of the programmed feed rate

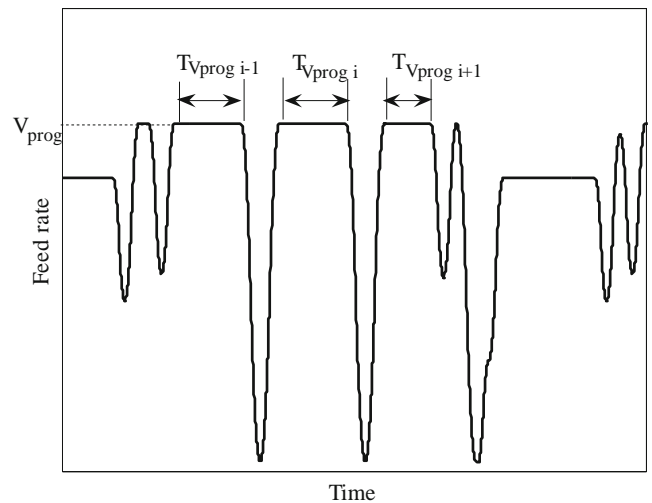


Fig. 25 Feed rate profile

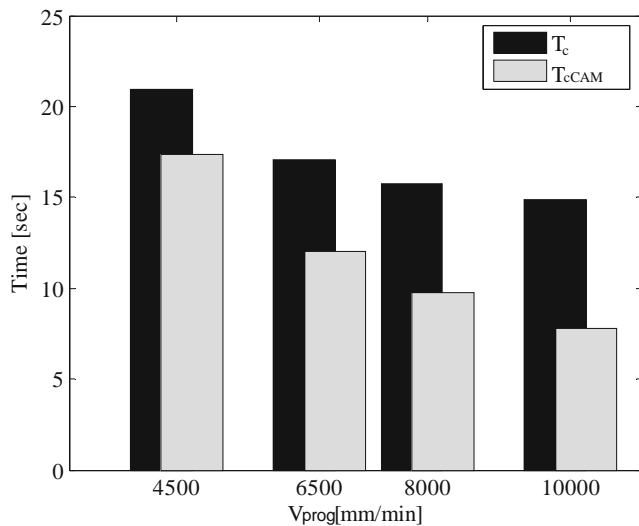


Fig. 26 Comparison of cycle time

4 Conclusion

This paper presents a theoretical study of the feed rate evolution in HSM for a circular interpolation. This work allows to presents a model of the machine tool behavior during a circular–circular interpolation. This model permits to determine the optimal fillet radius value which will be inserted at a discontinuity. This study can be associated with modeling a set of interpolations of a machining strategy.

For a fixed error ε , the model permits to calculate the fillet radius R_c and the TIT. An experimental study was carried out in order to validate models and to determine the influence of the geometry of the path on the feed rate evolution.

By comparing theoretical model and experimental study, a maximum error of 5 % was obtained. The industrial application permits to validate the modeling and to determine the influence of feed rate variation on the cycle time.

Future work will concentrate on developing a module for generating the trajectory according to the diameter of the tool. This module will be integrated in the used simulator. As a result, this simulator will be able to determine the optimal strategy and optimal tool diameter in order to minimize cycle time according to the machining quality. So, it can be applied to the pocket in any shape and mold machining.

Acknowledgments The authors gratefully acknowledge the valuable help rendered by SIAF manufacture during the course of the experimental study.

References

- Siller H, Rodriguez CA, Ahuett H (2006) Cycle time prediction in high-speed milling operations for sculptured surface finishing. *J Mater Process Technol* 174:355–362
- Souza AF, Coelho RT (2007) Experimental investigation of feed rate limitations on high speed milling aimed at industrial applications, *Int J Adv Manuf Technol* doi:10.1007/s00170-006-0445-2
- Sinumerik (2006) 840Dsl/840Disl/840D/840Di/810D Manuel de programmation Notions de base
- Pateloup V (2005) Amélioration du comportement cinématique des machines outils UGV—Application au calcul de trajets d'évidement de poches, Phd thesis, Blaise Pascal–Clermont II University
- Dugas A (2002) Simulation d'usinage de formes complexes, Phd thesis, IRCCYN, Ecole Centrale Nantes
- Pessoles X (2010) Aide au choix du posage en usinage 5 axes continus par la modélisation du comportement cinématique des machines—outils, Phd thesis, Université Toulouse 3 Paul Sabatier (UT3 Paul Sabatier)
- Tapie L, Mawussi BK, Anselmetti B (2007) Circular tests for HSM machine tools: bore machining application. *Int J Mach Tool Manuf* 47:805–819
- Moneral M, Rodriguez CA (2003) Influence of tool path strategy on the cycle time of high-speed milling. *Comput-Aided Des* 35:395–401
- Coelho RT, Souza AF, Rodrigues Roger A, Yoshida Rigatti AM, Ribeiro AL (2009) Mechanistic approach to predict real machining time for milling free-form geometries applying high feed rate, *Int J Adv Manuf Technol*, doi:10.1007/s00170-009-2183-8
- Zhao ZY, Wang CY, Zhou HM, Qin Z (2007) Pocketing tool path optimization for sharp corners. *J Mater Process Technol* 192–193:175–180
- Pateloup V, Duc E, Ray P (2004) Corner optimization for pocket machining. *Int J Mach Tool Manuf* 44:1343–1353
- Held M, Spielberg CH (2009) A smooth spiral tool path for high speed machining of 2D pockets. *Comput-Aided Des* 41:539–550
- Sai L, Bouzid W, Zghal A (2008) Chip thickness analysis for different tool motions for adaptive feed rate. *J Mater Process Technol* 204:213–220
- Kloypayan J, Lee YS (2002) Material engagement analysis of different end mills for adaptive feed rate control in milling process. *Comput Ind* 47:55–76
- Erkorkmaz K, Altintas Y (2001) High speed CNC system design. Part I: jerk limited trajectory generation and quintic spline interpolation. *Int J Mach Tool Manuf* 41:1323–1345